Int J Pharm Bio Sci 2014 Jan; 5(1): (P) 594 - 605

Research Article **Nanotechnology**

International Journal of Pharma and Bio Sciences

ISSN 0975-6299

MODIFIED SWITCHING CHARACTERISTICS OF CARBON NANOTUBES BLENDED WITH TYPE II CdTe QUANTUM DOTS

A WATTS[1], M GREEN[2], A WAHEED[1,3]*, S.K. CHAKARVARTI[4] AND M FARMER[1]

1British Institute of Technology & E-commerce ,Avicenna House, 258-262 Romford Road, London E7-9HZ, The United Kingdom
2 Department of Physics, King's College London, Strand, London WC2R 2LS, The United Kingdom
3 Cranford College London, 680 Bath Road,Hounslow, Middlesex TW5 9QX,The United Kingdom
4 Manav Rachna International University (MRIU), Faridababd,Haryana, India

ABSTRACT

We have investigated the electrical properties of the hetero structures deposited on conductive glass. The hetero structures made with type II CdTe quantum dots present interesting peculiarities. Low frequency (20Hz ≤ f≤ 200kHz; f= 8804) dielectric properties of type II CdTe, type II CdTe blended with Single-wall carbon nano tubes SWNTs functionalized with poly (ethylene glycol) hetero junctions, were investigated in details at room temperature. Negative capacitance was observed at low frequencies under forward dc biases. . By using frequency dependent capacitance spectroscopy, the tunnelling effects of holes and electrons were investigated. Peaks were observed In capacitance curves measured at low frequency, which could be attributed to the resonant tunnelling of charge carriers into discrete energy levels of nanocrystalline CdTe and exhibit quantum confinement and coulomb blockade effects. A clear (positive/negative) shift in capacitance-voltage(C-V) and conductance-voltage (G-V) suggests (electron/hole) trapping in nanocrystalline quantum dots.

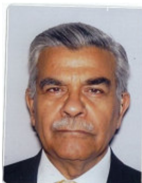

A WAHEED
Cranford College London, 680 Bath Road,Hounslow, Middlesex TW5 9QX,The United Kingdom

***Corresponding author**

1. INTRODUCTION

The nearly perfect structure of carbon nanotubes(CNTS) put them in a good position as candidates to go beyond the silicon based technology in down-scaling of electronic components((1-4). The hysteresis often displayed in CNT devices such as carbon nanotube field-effect transistor (CNTFET) is a challenge in the transfer characteristics (5). However, on the other hand, this hysteresis can be utilized as a memory device with the added dimension of illumination-enhanced switching (6). Different methods were used to produce CNT based memory devices, for example, using ferroelectric materials has been done since 1950(7-10), and recently metal-ferroelectric-metal-insulator-semiconductor FET (MFMSFET) (11). Using hydrogen and air annealing was used to produce a pronounced hysteresis loop (12). A proper control of the surface charges is necessary for practical applications. Ferroelectric (11) materials were used with single wall carbon nanotubes (SWNTs) in producing Memory devices in transistor form (6,12,13,14) or diode form (15). Here we report our study of a diode stability in these systems having an associated memory phenomenon, using CdTe type II blended with SWNTs functionalized with poly (ethylene glycol) .

2. Experimental Procedure

The devices prepared and studied consist of a thin layer of CdTe type II quantum dots or a mixture of CdTe with single wall carbon nanotubes (poly(ethylene glycol)functionalized) sandwiched between two electrodes (ITO-Indium Tin Oxide) and Al on top of a glass substrate. The mixture is spin coated on top of an optically transparent ITO electrode, after spin coating the ITO with PEDOT : PSS conductive polymer which is a mixture of two ionomers poly (3,4-ethylenedioxythiophene) and poly (styrenesulfonate). One component PSS in this mixture is made up of sodium polystyrene sulfonate which is a sulfonated polystyrene. Part of the sulfonyl groups are deprotonated and carry a negative charge. The other component poly (3,4-ethylenedioxythiophene) or PEDOT is a conjugated polymer which carries positive charges and is based on polythiophene The high work function of PEDOT :PSS makes it suitable for hole injection. In this case the top electrode evaporated Al is used, which has a low work function and serves as the electron injector. The ferroelectric property was characterized at room temperature by using a modified Sawyer-Tower circuit (16). This ferroelectric behaviour can be attributed to the interaction induced ferro-electricity in polar molecules (17). The current –voltage (I-V) characteristics were obtained with the positive voltages corresponding to a reverse bias. By analogy, the negative voltages correspond to a forward bias.

3. RESULTS AND DISCUSSION

The conduction mechanism was studied under different conditions of current and voltage. Fig.1 shows the current-voltage characteristics. The poor quality of the diode is reflected in its slope that is significantly far from unity. The reverse bias shows a slight kink at a voltage around 1.5V (Fig.1). As the I-V characteristic is asymmetric with respect to positive and negative voltages (as is usually the case), the injection process is most probably Schottky injection. Fig.2 presents typical I-V plot showing increased current through the junction due to the onset of Fowler-Nordheim Tunneling (FN tunneling).It is found that the FN plot for a semiconductor has the nonlinear slope that originates in the emission mechanism. The slope of the FN plot has three values, each value representing the slope in the three distinct regions of field. This implies that the tunneling probability makes three distinct contributions to the electron emission. The slope is modified with the carrier concentration and the band gap. For carbon nanotubes the FN theory often breaks down with the current showing saturation at high fields, or with two distinct Fowler-Nordheim slopes (18). The plot in Fig.3 shows the two distinct plots. In the low-voltage region the emission is produced at a very low voltage which suggests that the FN equation fails to accurately model the emission at least for low

fields below a knee voltage, V_{knee} , The V_{knee} is a breakpoint at which the emission data deviate from the low-voltage, straight- line asymptote. In the high - voltage region above $V_{knee.}$, the data of Fig.3 give a near straight-line fit. The failure of the FN model in describing the emission at low voltages is accounted for by incorporating additional interactions since the FN plot is just an approximation of a more complex emitting behaviour. Since at low fields there is no FN tunneling , i.e., no “thinning” of dielectric, so direct tunneling is mainly responsible for the conduction in a similar manner to the 45nm transistor(19). This can be attributed to the random alignment of CNT clusters. One explanation of the observed behaviour could be: at lower electric field, emission occurs only from the nearest CNT to the anode. This leads to a smaller emission area with very high field enhancement factor β, leading to the observed lower current but a shallow FN slope. At higher electric fields, more CNT in the cluster are able to emit. This leads to a higher emission area and hence the observed high current with a steep FN slope. Another reason for the different levels of charge carrier emission from CNT is the tube height according to the observations of Suh et al (20), they found that the emission is optimal when the height of the CNTs is similar to the intertube distance which is not the case with the CNTs we used here length 0.5-0.6µ m intertube distance in nms (Sigma Aldrich), their conclusion was with an increase in tube height, the aspect ratio of the tube height to the radius will produce efficiency that will increase with relatively low aspect ratios. The knee in Fig.3 can be attributed to the onset of hole tunneling which change the sign or direction of the current due to hole injection (21, 22).

The switching mechanism was further studied using an alternating - current impedance. This increase in capacitance at low frequency may be due to the increase in the apparent dielectric constant of the insulator in the active layer which is associated with the field-induced dipole formation (23). There is also a noticeable difference between the ramp up and ramp down value of the capacitance at the low frequency Fig.4 .Since no DC bias was applied to the junction the switch simply followed the applied square or triangular wave ac signal. Due to this several stages where observed when the device was switched from full on to off states. At this stage we did not try to address the different states in a controllable way. The phenomenon of space charge polarization appeared and a large dielectric relaxation was observed Fig.4. The impedance shows a relaxation occurring above 10^5Hz as shown in Fig.5. At high frequencies, the a.c. conductance, G, results from the displacement current contribution. For the pristine sample capacitance C and conductance G vs frequency with no bias is shown in Fig.6 (a) with the lowest conductivity in the forward ramp up arrangement, and higher values in the reverse both in the ramp up and ramp down arrangement in Fig. 6(b,c). The frequency response was examined after raising the voltage. Fig.7 shows C and G under steady state conditions at dc voltage of 5 V. The C and G data are identical in the voltage range 1V till 4.5V.When the dc bias exceeds 4.5V the low frequency capacitance decreases and changes (at certain CNT concentration and pure CdTe QDs)sign becomes an inductance with the effect of the appearance of this inductance at different frequencies with changing concentration of CNT. This “negative capacitance” (inductance) indicate that the current variation lags behind the voltage agitation. The negative capacitance behaviour has been observed in a nanoscale based solar cell (24) and has also been observed at low frequencies in p-i-n junctions made from amorphous silicon (25).Since the ionic contribution is significant only at low frequencies the g response persists to much higher frequencies .This G results from the injected charge carriers (electrons and holes). There are two main types of interpretations suggested for the negative capacitance (or inductive behaviour). In the short-base p-n junction, the minority carrier depopulation at high forward bias induces a change of sign of the capacitance (26, 27, 28). But a general interpretation of the negative capacitance (inductive) mechanism takes place when the current between two electronic reservoirs is governed by the occupation of an intermediate state, which decreases when the applied potential

increases. In the case of Schottky diodes the negative capacitance was due to the interface charge loss at the occupied states below Fermi level (29). In the case of double –barrier resonant tunneling diode (RTD), the quantum capacitance becomes negative in the region of negative differential resistance due to the electron charges decrease at increasing forward bias (30, 31). A ferroelectric-like hysteresis loop is presented in Fig.8, with the loop visible between 1985 Hz to 465 kHz, to study the hysteresis and switching behaviour.. The hysteresis is due to the non centrosymmetric nature of the compounds used in the blend. At low frequencies, the hysteresis can be accommodated through proportional – integral - derivative (PID) .However, at higher frequencies, increasing noise-to data ratios and diminishing high-pass characteristics of control filters preclude a sole reliance on feedback laws to eliminate hysteresis. Alternatively, the use of charge – or current-controlled amplifiers can eliminate hysteresis. However, this mode of operation can be prohibitively expensive. This motivates the development of models and model based control designs which incorporate and accommodate the hysteresis. One technique which is based on the homogenized energy models (32, 33), this led to the exact or approximate inverse model to linearized the transducer behavior (34) in the manner depicted in Fig.3. Besides the challenge that CNTs often display some degree of hysteresis, on the other hand, the presence of the hysteresis loop open up the possibility of utilize the device in a memory component. Switching behaviour: In Fig.9 a series of square wave pulses were applied to the junctions with the response recorded on a different channel. The stability of the switching characteristics is dependent on the peak voltage and frequency of the applied pulses. For a further investigation of the switching characteristics we performed dc current-voltage measurement. In Fig.10 the current-voltage (I-V) characteristics are shown for a dc voltage ranging from 0→1 volt. At the switching voltage of 0.8 volt, the current drastically increases in magnitude.

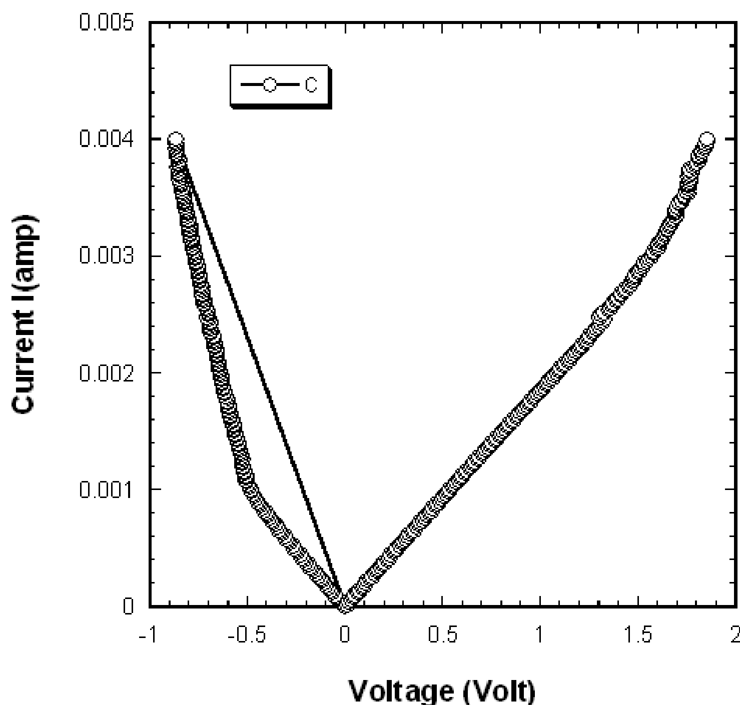

Figure 1
Current-voltage plot of ITO/CdTe/CdS/ZnS Core/shell/shell quantum dots +SWNT (polyglycol functionalized) spincoated/Al.

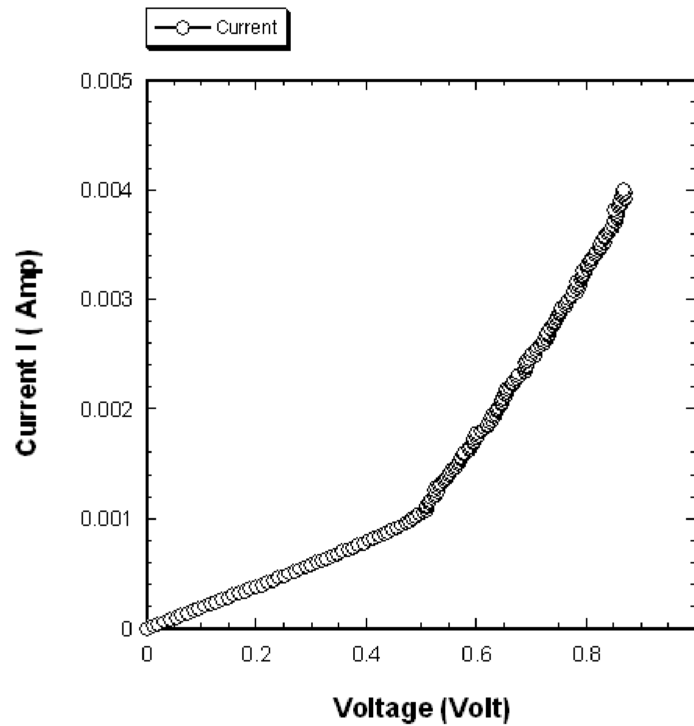

Figure 2
Reverse Current-Voltage plot of ITO/CdTe/CdS/ZnS Core/shell/shell quantum dots +SWNT (poly ethyleneglycol functionalized) spincoated /Al.

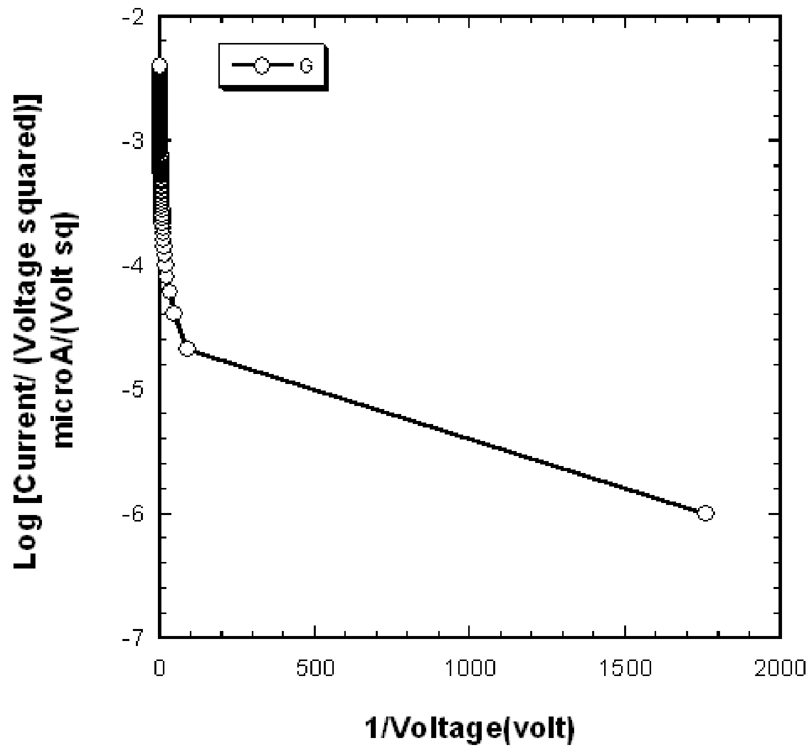

Figure 3
Fowler-Nordheim plot of ITO/CdTe/CdS/ZnS Core/shell/shell quantum dots +SWNT (poly ethyleneglycol functionalized) spincoated /Al.

This article can be downloaded from www.ijpbs.net

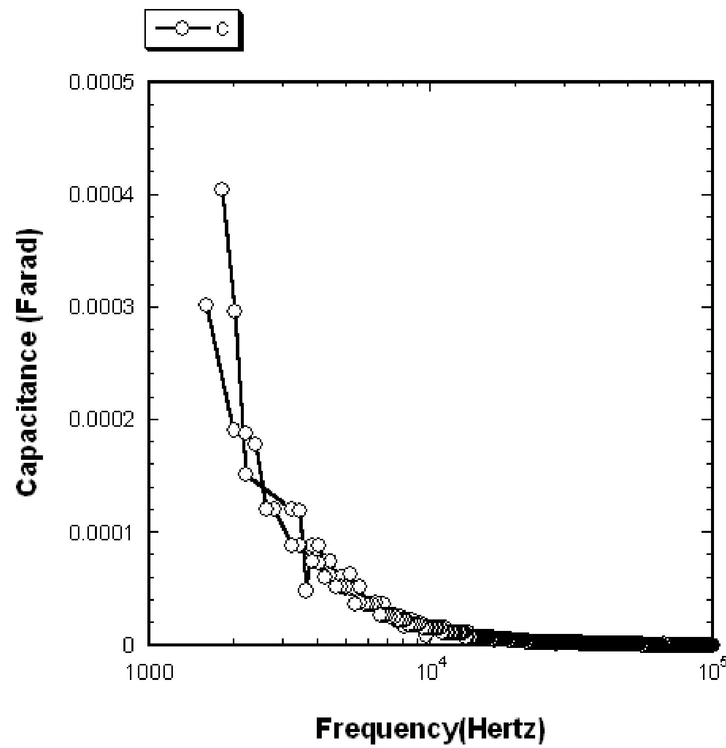

Figure 4
Capacitance-frequency plot of ITO/CdTe/CdS/ZnS Core/shell/shell quantum dots +SWNT (poly ethyleneglycol functionalized) spincoated /Al with 1.5V bias.

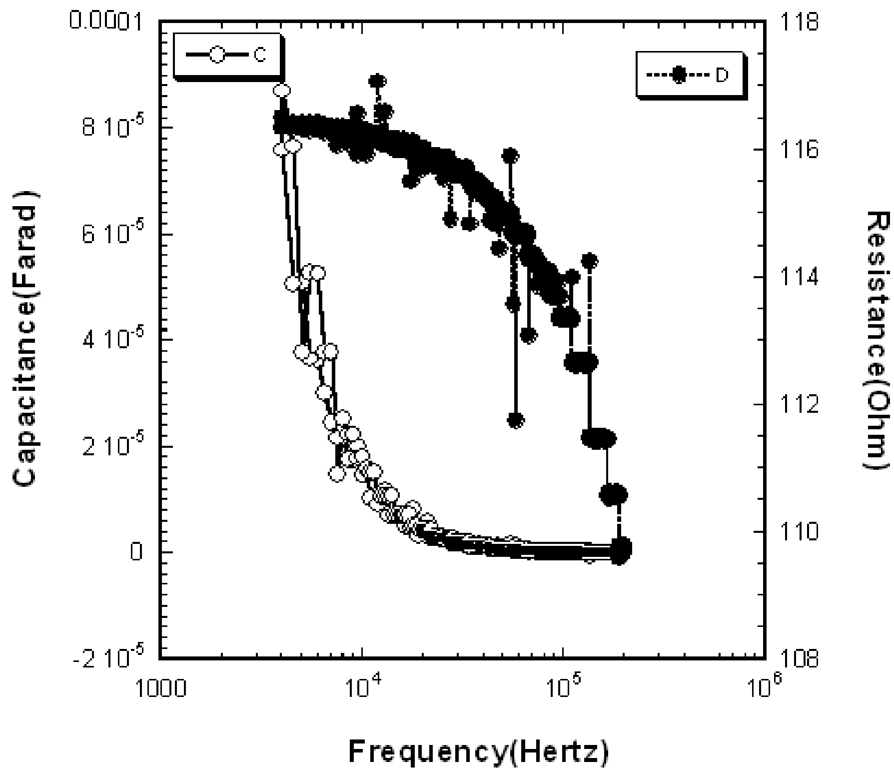

Figure 5
Capacitance-frequency plot of ITO/CdTe/CdS/ZnS Core/shell/shell quantum dots +SWNT (poly ethyleneglycol functionalized) spincoated /Al with 3V bias.

This article can be downloaded from www.ijpbs.net

Figure6a

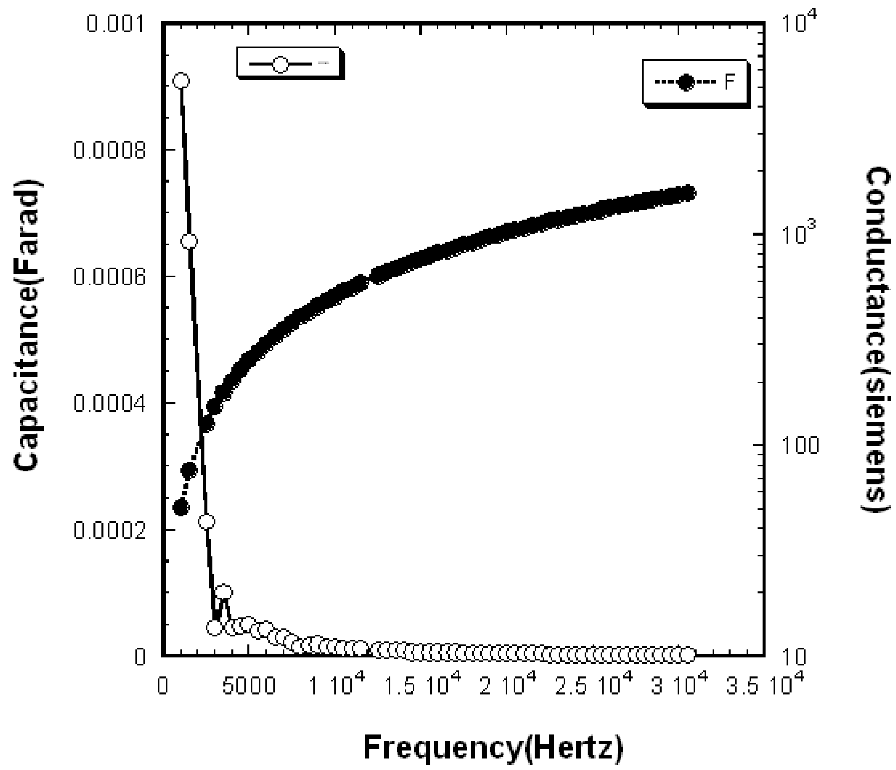

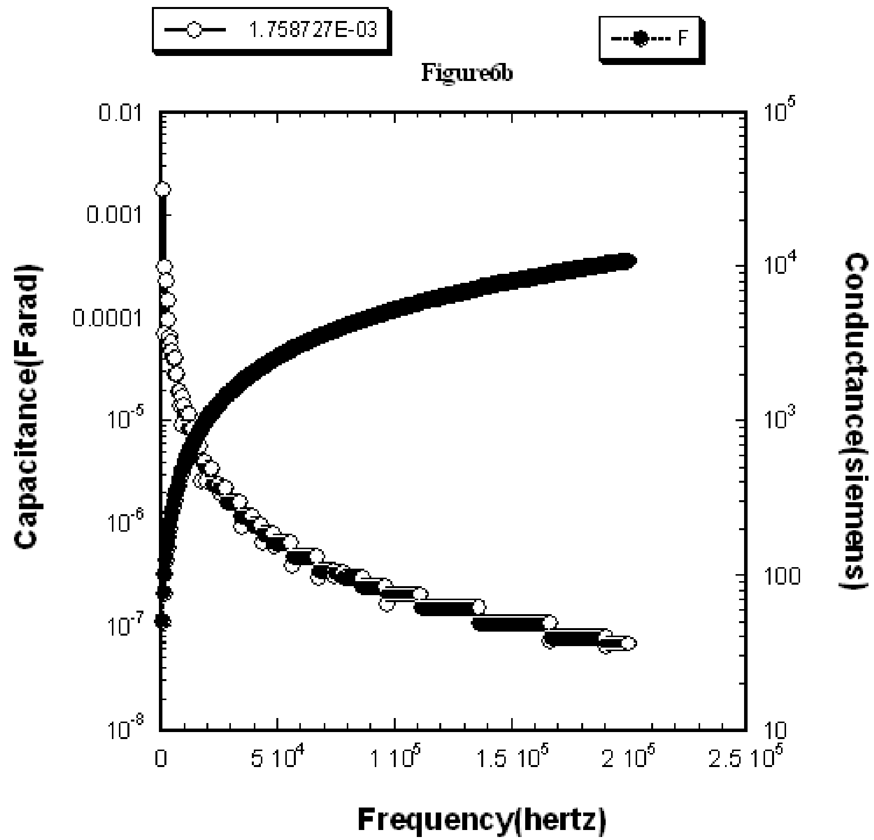

Figure6b

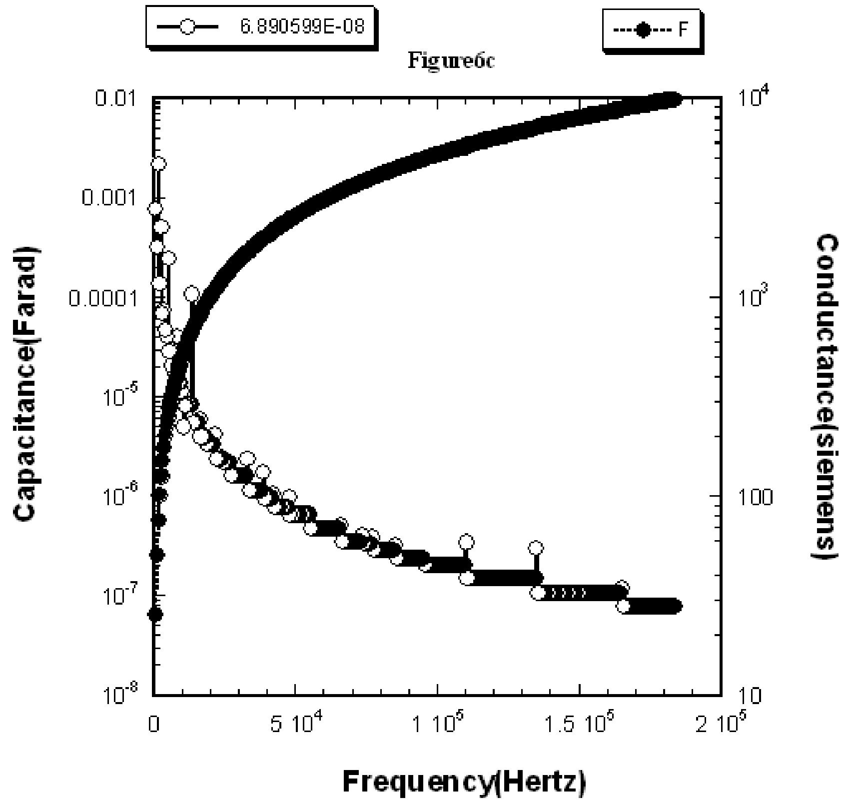

Figure 6
Capacitance-frequency plot of ITO/CdTe/CdS/ZnS Core/shell/shell quantum dots +SWNT (poly ethyleneglycol functionalized) spincoated /Al with no bias.

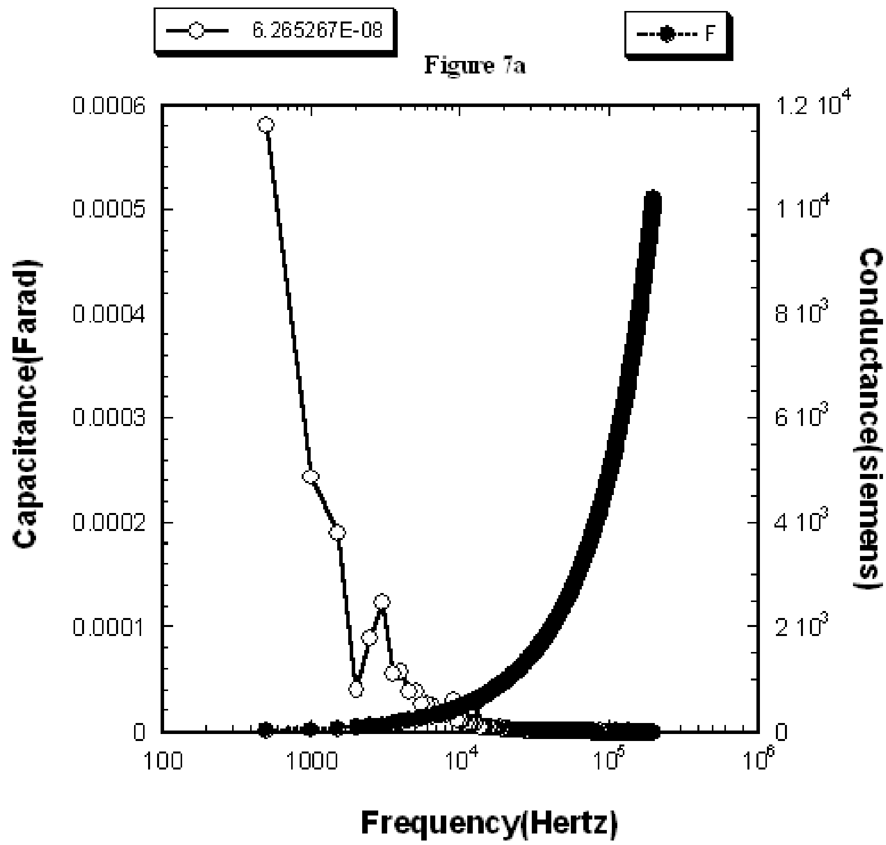

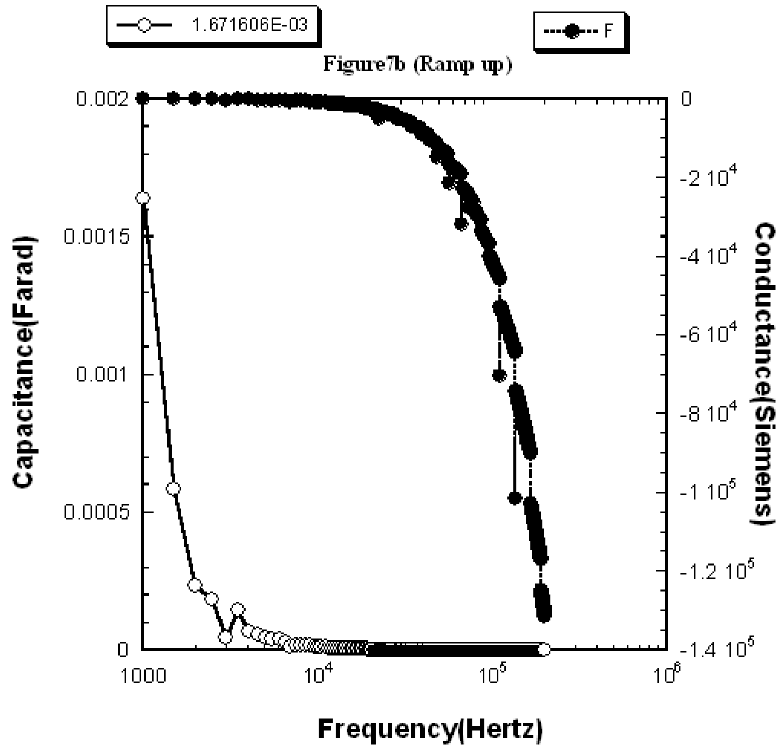

Figure 7
Capacitance-frequency plot of ITO/CdTe/CdS/ZnS Core/shell/shell quantum dots +SWNT (poly ethyleneglycol functionalized) spincoated /Al with 5V bias.

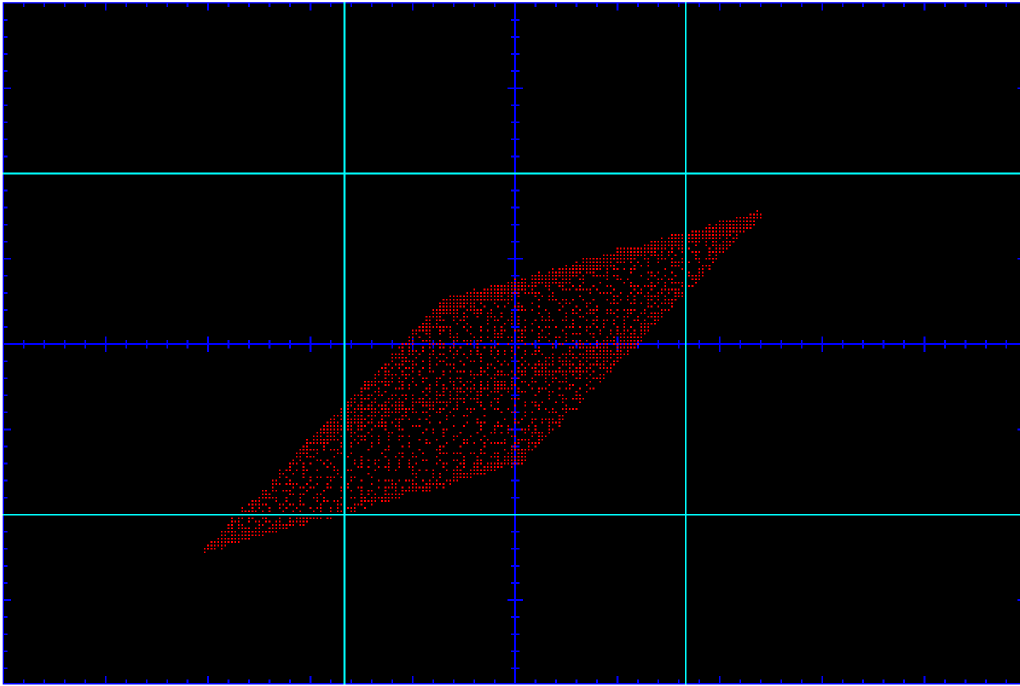

Figure 8
Hysteresis Loop of ITO/CdTe/CdS/ZnS Core/shell/shell quantum dots +SWNT (poly ethyleneglycol functionalized) spincoated /Al.

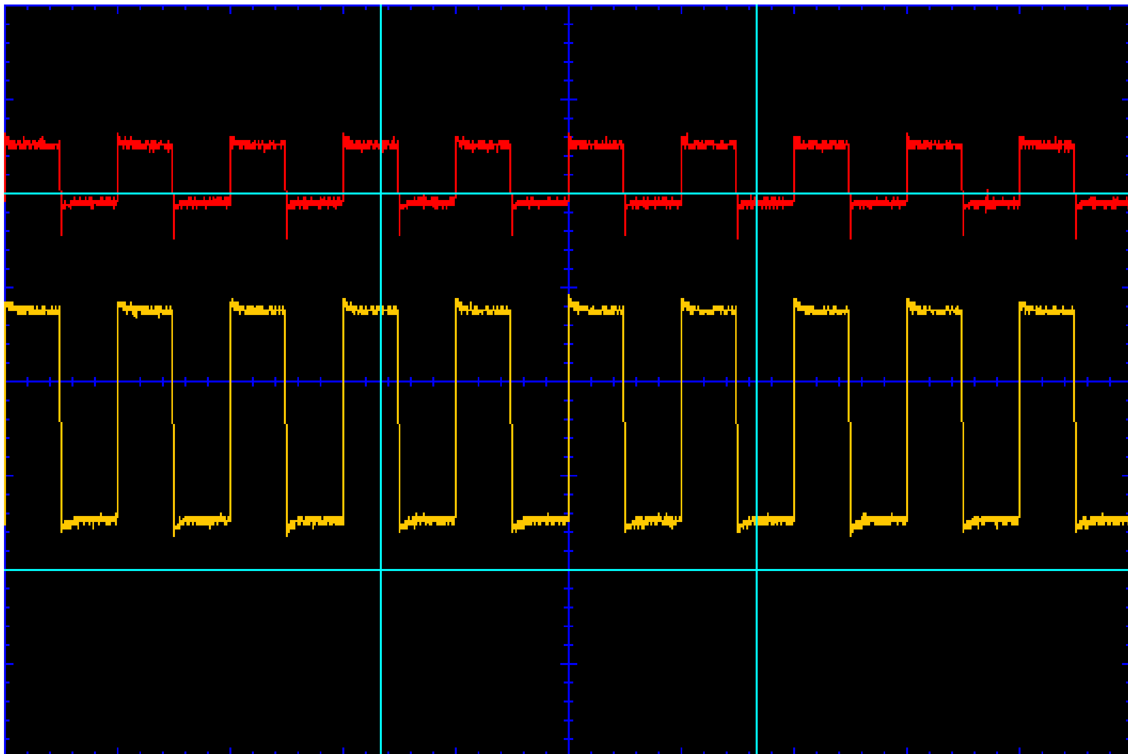

Figure 9
Digital storage Oscilloscope Output for the device cycling using trains of voltage sequence. The top and bottom curves are the corresponding current response and the applied voltage.

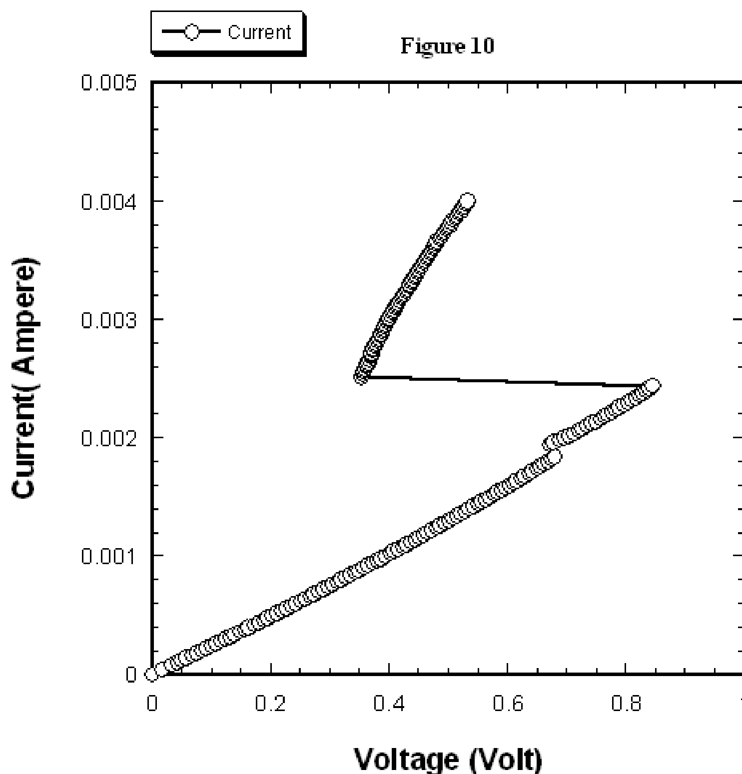

Figure 10
Current-voltage of ITO/CdTe/CdS/ZnS Core/shell/shell quantum dots +SWNT (poly ethyleneglycol functionalized) spincoated /Al showing switching behaviour.

4. CONCLUSION

Our experimental results show hysteretic diode characteristics of a ferroelectric-like loop. This behaviour is brought about by the blends of electronically interacting composite systems based on (CNT) and chalcogenide-based CdTe quantum dots, have shown signs as an electrical bistable device. The composite systems, because of their size, can be a potential memory element. The bistability in these systems has an associated memory phenomenon. The transition between the two conducting states are rewritable in nature and may have RAM (Random Access Memory) applications. This is an important topic for research requiring in depth understanding of the carbon structures like carbon nanotubes having the cage-like architecture (35). It may further be suggested that, to proceed with this kind of research, one should consider giving due preference to the application of track etch technology. Faster etching along the heavy ion produced cores lead to pores of various sizes. This technique makes it possible to produce nanostructures (nanowires and nanotubes) for a broad variety of high technology application in the fast growing nanotechnology markets. Because of the highly ordered nature of nanowires, they can be directly patterned for fabrication of nanodevices (36). This is related to the possibility of using modified individual non-overlapping latent tracks as future electronically active elements of nano-metric dimensions in large scale electronic devices (37)

ACKNOWLEDGEMENT

This experimental part of this work was carried out and completed at the nano - laboratory of British Institute of Technology and E - Commerce (BITE) under the supervision of Dr. M. Farmer. The authors appreciate all material

and moral support provided by BITE to complete this work. Thanks are due to Mr. K. Sarwar. The Chairman Cranford College London for financial support. The technical help provided by the staff of Cranford College London in preparing the script is acknowledged with thanks.

REFERENCES

1. A.G.Rinzler,J.H.Hafner,P.Nikolaev,L.Lou,S.G.kim,D.Tomanek, P.Nordlander,D.T.Colbert and R.E.Smalley; Science 269,1550(1995).
2. R.Martel,T.Schmidt,H.R.Shea,T.Hertel, and Ph.Avouris; Appl.Phys.Lett. 73,2447(1998).
3. S.J.Tans,A.R.M.Verschuren and C.Dekker;Nature (London) 393,49 (1998).
4. H.W.C.Postma,T.Teepen,Z.Yao,M.Grifonian d C.Dekker; Science 293,76(2001).
5. H.Shimauchi,Y.Ohno,S.kishimoto and T.Mizutani; Jap.J.App.Physics 45, 5501 (2006)
6. C.W.Lee,X.Dong,S.H.Goh,J.Wang,J.Wei andLJ.Li; J.Phys.Chem.C.Letters 113, 4745 (2009)
7. D.H.Looney,U.S.PatentNo2,791,758(1957); W.L.Brown,U.S.PatentNo2,791,759(1957);J. A.Morton,U.S.Patent No2 791,761(1957)
8. Advanced Microelectronics,edited by J.F.Scott(springer),Berlin,2000.
9. Auciello,J.F.Scott,and R.Ramesh ; Phys Today 51, 22(1998)
10. C.H.Ahn,J.M.Triscone,N.Archibald,M.Decroux,R.H.Hammomd,T.H.Geballe,F.Fischer and M.R.Beasley;Science 269,373(1995)
11. N.A.Basit and H.K.Kim; Appl.Phys.Letts.73,3941(1998)
12. S.Wang and P.Selling; App.Phys.Letts.87,133117(2005)
13. J.W.Cheah,Y.Shi,H.G.Ong,C.W.Lee,L.Li and J,Wang; Appl.Phys.Letts.93,082103(2008).
14. W.Fu,Z.Xu,X.Bai,C.Gu and E.Wang; Nanoletters l9,921 (2009)
15. J.Yao,Z.Jin,L.Zhong,D.Natelson and J.M.Tour; ACS Nano 3,4122 (2008)
16. R.C.G.Naber,C.Tanase,P.W.M.Blom,G.H.Gelinck,A.W.Marsmon,F.J.Touwslager,S.Setayesh,D.M.de Leeuw; Nat.Mater.4,243 (2005)
17. C-H.Lin,Y-T.Hsu,H.Lee and D - W. Wang; Phys Rev. A 81, 31601 (2010)
18. P. G. Collins, A. Zettl, Phys. Rev. B55, 9391 (1997)
19. J. Hicks et al ; Intel Technology Journal 12, 131 (2008)
20. J.S.Suh,k.S.Jeong,J.S.Lee and I.Han; App. Phys. Letts 80 ,2392 (2002)
21. Y.T.Hou,M.F.Li,Y.Jin and W.H.Lai; J.App.Phys 91, 258 (2002)
22. I.D.Parker; J.Appl.Phys 75, 1656 (1994)
23. C.W.Chu,J.Ouyang,J-H.Tseng, and Y.Yang; Advanced Materials, 117, 1440 (2005)
24. I.Mora-Sero,J.Bisquert,F.Fabregat-Santiago, and G.Garcia-Belmonte, Nano Letters 6, 646 (2006)
25. F.Lemmi and N.M.Johnson; MRS Conference, San Francisco, April 13-17,1998.
26. Lindmayer J. , WrigleyC.Y. ; Fundamentals of Semiconductor Devices, Van Nostrand, New york,1965, p237
27. Van den Biesen, J.J.Hansen; Solid-state Electronics 33,1471 (1990)
28. Laux,S.E., Hess K. ; IEEE Trans. Electron Devices 46,396 (1999)
29. Wu,X., Yang E.S., Evans H.L; J.Appl.Phys. 68,2846 (1990)
30. Hu Y., Stapleton S.P. ; Appl.Phys.Lett. 58,167 (1993)
31. Hu,Y., Stapleton,S.P. ; IEEE.J.Quantum Electron 29,327 (1993)
32. R.C.Smith ,A.Hatch, B.Mukherjee and S.Liu ; Journal of Intelligent Material Systems and Structures 18, 69 (2007)
33. R.C.Smith,S.Seelecke,Z.Ounaies and J.Smith ; Journal of Intelligent Material Systems and Structures14, 719 (2003)
34. A.G.Hatch,R.C.Smith,T.De,M.V.Salapaka; IEEE Transaction on Control Systems Technology 14, 1058 (2006)
35. M. Abhilash; Intern J. Pharma and Bio Sciences (IJPBS) 1, 1, (2010)
36. S. Kumar,D.Saini,G.S.Lotey,N.K.Verma; Superlattices and Microstructures 50, 698, (2011)
37. A.Waheed,G.R.Mitchell,P.J.F.Harris,M.Farmer,A.Watts,N.Shahzad, and K.Chakarvarti Intern J. Pharma and Bio Sciences (IJPBS) 3, 368, (2012)